Caspase-3-Dependent Apoptosis of Citreamicin ε-Induced HeLa Cells Is Associated with Reactive Oxygen Species Generation

ARTICLE *in* CHEMICAL RESEARCH IN TOXICOLOGY · JUNE 2013

Impact Factor: 3.53 · DOI: 10.1021/tx4000304 · Source: PubMed

Chemical Research in Toxicology

Article

pubs.acs.org/crt

Caspase-3-Dependent Apoptosis of Citreamicin ε-Induced HeLa Cells Is Associated with Reactive Oxygen Species Generation

Ling-Li Liu,[†] Li-Sheng He,[†] Ying Xu,[†] Zhuang Han,[†] Yong-Xin Li,[†] Jia-Liang Zhong,[‡] Xian-Rong Guo,[§] Xi-Xiang Zhang,[§] Kam Ming Ko,[†] and Pei-Yuan Qian*[,†]

[†]Division of Life Science, The Hong Kong University of Science and Technology, Clear Water Bay, Kowloon, Hong Kong SAR, China

[‡]Shanghai Institute of Pharmaceutical Industry, Shanghai 200040, P. R. China

[§]Advanced Nano-fabrication, Imaging & Characterization Core Laboratory, King Abdullah University of Science and Technology, Thuwal 23955-6900, Saudi Arabia

Supporting Information

ABSTRACT: Citreamicins, members of the polycyclic xanthone family, are promising antitumor agents that are produced by *Streptomyces* species. Two diastereomers, citreamicin ε A (**1**) and B (**2**), were isolated from a marine-derived *Streptomyces* species. The relative configurations of these two diastereomers were determined using NMR spectroscopy and successful crystallization of citreamicin ε A (**1**). Both diastereomers showed potent cytotoxic activity against HeLa (cervical cancer) and HepG2 (hepatic carcinoma) cells with IC_{50} values ranging from 30 to 100 nM. The terminal deoxynucleotidyl transferase dUTP nick-end labeling assay confirmed that citreamicin ε A (**1**) induced cellular apoptosis, and Western blot analysis showed that apoptosis occurred via activation of caspase-3. The 2,7-dichlorofluorescein diacetate assay indicated that citreamicin ε substantially increased the intracellular concentration of reactive oxygen species (ROS). To confirm the hypothesis that citreamicin ε induced apoptosis through an increase in the intracellular ROS concentration, the oxidized products, oxicitreamicin ε A (**3**) and B (**4**), were obtained from a one-step reaction catalyzed by Ag_2O. These products, with a reduced capacity to increase the intracellular ROS concentration, exhibited a significantly weakened cytotoxicity in both HeLa and HepG2 cells compared with that of citreamicin ε A (**1**) and B (**2**).

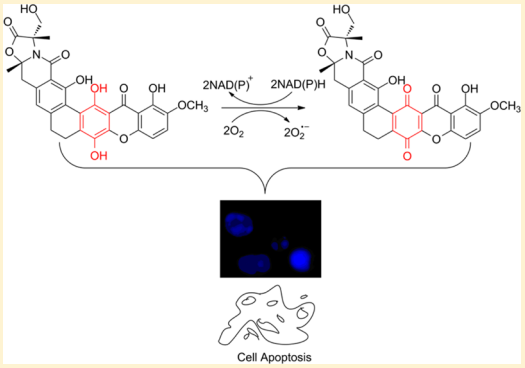

INTRODUCTION

Citreamicins belong to the polycyclic xanthone family and are promising antitumor agents. These compounds were first isolated from *Streptomyces*,[1] a group of Gram-positive bacteria that is well-known for producing fused-ring aromatic polyketides. The basic carbon skeleton of citreamicins consists of seven condensed rings, including six polycyclic aromatic rings and an oxazolidone ring. To date, 12 citreamicins have been reported, with some displaying strong cytotoxic activity.[2−5] However, the mechanisms underlying the cytotoxicity of citreamicins have not been investigated.

Apoptosis, or programmed cell death, is important for maintaining the normal physiological functions of a biological organism.[6] Apoptosis, which can be triggered via various stimuli, is characterized by DNA damage, chromatin condensation, and cell shrinkage in the early stage, followed by nuclear and cytoplasmic fragmentation.[7,8] There are two important biomarkers of cell apoptosis: activated caspases and DNA fragmentation.[9] Caspases are cysteine-dependent aspartate-specific proteases, including caspase-3, caspase-8, and caspase-9. Caspase activation plays an important role during apoptosis; in particular, the activation of caspases-3 is a critical step in this process.[10] Irrespective of the extrinsic pathways initiated by the Fas/Fas ligand system or the intrinsic pathway mediated by mitochondria, both of these apoptotic pathways converge to activate the downstream executioner caspases-3.[11]

Reactive oxygen species (ROS) collectively describe O_2-derived free radicals such as hydrogen peroxide (H_2O_2).[12] ROS have been implicated in the regulation of many important cellular events such as apoptosis.[13] A growing body of evidence has implicated ROS in triggering, mediating, and executing apoptosis. ROS production induces the oxidative modification of cellular macromolecules, inhibits protein functions, and promotes cell apoptosis.[14,15] The functional role of ROS in the induction of apoptosis has been studied in many systems.[16,17] Several research groups have shown that natural products, such as hydroquinone[18] and pyridoacridines,[19] induce cell apoptosis through an increase in the extent of ROS generation.

The strain *Streptomyces caelestis* was isolated from the coastal water of the Red Sea and characterized as possessing extraordinary cytotoxicity against HeLa cells in preliminary

Received: January 21, 2013
Published: May 22, 2013

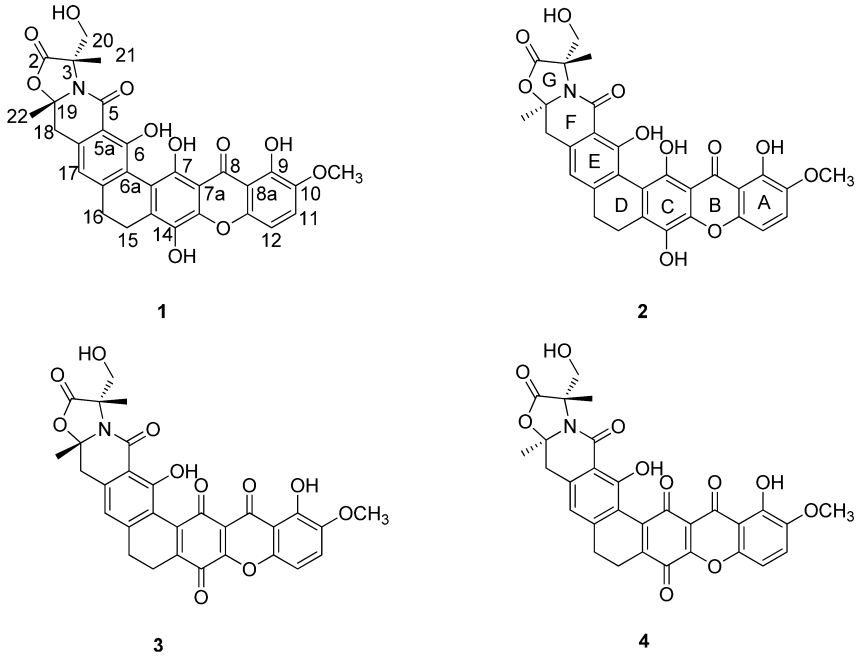

Figure 1. Chemical structures of the two diastereomers, citreamicin ε A (**1**) and B (**2**), and their corresponding oxidized products, oxicitreamicin ε A (**3**) and B (**4**), respectively.

screening tests. When this strain was grown in a flask with glass beads, its ethyl acetate (EA) extract showed a high level of cytotoxic activity, even at a low concentration (Figure S1 of the Supporting Information). The bioassay-guided fractionation of *S. caelestis* facilitated the extraction and isolation of citreamicin ε. Although this compound has been isolated and a similar structure has been patented as a potential candidate for anticancer drug discovery,[20] neither the stereochemistry nor the cytotoxic mechanism of this compound has been studied. In this study, we resolved the two diastereomers of citreamicin ε using crystallization and compared the cytotoxicity of these compounds in different cell lines. We also evaluated the potential cytotoxic mechanism of citreamicin ε that involved caspase-3-dependent apoptosis. We found that ROS might be responsible for the toxicity of citreamicin ε, as this compound could induce a substantial increase in the level of intracellular ROS. To validate the involvement of ROS in apoptosis, we modified the structure of citreamicin ε to obtain the oxidized product, oxicitreamicin ε. A comparison of the cytotoxic activity of citreamicin ε and oxicitreamicin ε indicated that ROS generation was involved in apoptosis. Here, we report the fermentation, isolation, elucidation of the structure, cytotoxic activity, and potential cytotoxic mechanism of citreamicin ε.

EXPERIMENTAL PROCEDURES

Microbial Material and Sample Collection. Strain AW9-9C was isolated from the Red Sea coastal waterside of a fish market near Jeddah (21′29.622″ N 39′9.617″ E). The pure culture was isolated with Actinomycete Isolation Agar 212168 (BD Difco). Total genomic DNA was prepared using a previously described method.[21] The 16S rDNA (1575 bp long) similarity of this strain was assessed using the BLAST program in the NCBI Database.[22] The strain was classified as *S. caelestis* according to the 16S rDNA sequence (99% similar), which was submitted to GenBank as accession number JX204833.

Fermentation, Extraction, and Isolation. *S. caelestis* was fermented in SPY medium [starch (10 g/L), peptone (2 g/L), yeast extract (4 g/L), and sea salt (20 g/L)] at 23 °C, while being shaken at 160 rpm for 5 days. The seed culture (2.8 L) was used to inoculate 37 flasks (2.8 L) containing 1 L of the medium and approximately 100 glass beads. Subsequently, the culture was filtered and the broth extracted using EA, and the mycelia were extracted using acetone and methanol [1:2 (v/v)]. The broth and mycelia extracts were combined and partitioned three times between water and hexane. The aqueous layer was further extracted using EA. A large amount of insoluble powder was obtained after the EA fraction had been dried under a vacuum. The insoluble powder was dissolved in dimethyl sulfoxide (DMSO), subjected to semipreparative reversed phase HPLC, and eluted with a MeOH/H_2O mixture containing 2.0 g/L NH_4OAc at 40 °C, using an increasing gradient of MeOH from 50 to 100% over 20 min to afford citreamicin ε A (**1**) and B (**2**) (Figure 1).

Chemical Structure Analysis. Optical rotation was performed using a Perkin-Elmer model 241 polarimeter. Circular dichroism (CD) spectra were measured on a Chirascan instrument, and infrared spectra (IR) were measured using a Bio-Rad FTS-135 spectrometer with KBr pellets. ^1H, ^{13}C, and two-dimensional (2D) NMR spectral data were obtained using Varian Inova 500 MHz NMR spectrometers. Electrospray ionization (ESI) and high-resolution mass spectra were acquired using an UPLC-TOF-MS system. The UPLC system comprised a Waters ACQUITY UPLC system (Waters, Manchester, U.K.) coupled to a Bruker micrOTOF II mass spectrometer (Bruker Daltonics GmbH, Bremen, Germany). The X-ray diffraction study was performed using a Bruker SMART APEX-2 CCD, and the powder diffraction analysis was performed using Bruker D8 ADVANCE.

X-ray Crystallographic Analysis of Citreamicin ε A (1).[23] $C_{30}H_{25}NO_{11}$, M_r = 575.51, orthorhombic, space group $P2_12_12_1$, a = 8.197(2) Å, b = 14.197(3) Å, c = 21.934(4) Å, V = 2552.3(9) Å^3, Z = 4, d_x = 1.498 Mg/m^3, $F(000)$ = 1200, μ(Cu Kα) = 0.976 mm^{-1}. The data were collected with a Bruker SMART APEX-II using graphite-monochromated radiation (λ = 1.54178 Å), and 2882 unique reflections were collected to θ_{max} = 67.65°, where 4395 reflections were observed [$F^2 > 4\sigma(F^2)$]. The structures were determined using direct methods (SHELXTL, 2008) and refined using full-matrix least-squares analysis on F^2. The final values were as follows: R = 0.0471, R_w = 0.1308, and S = 1.006.

Cell Culture. Cervical cancer (HeLa) and hepatic carcinoma (HepG2) cells were obtained from ATCC (Manassas, VA) and maintained via adhesion on Petri dishes containing Dulbecco's modified Eagle's medium (DMEM) supplemented with 10% fetal bovine serum (FBS), 3% antibiotic and antimycotic solution [10000

dx.doi.org/10.1021/tx4000304 | Chem. Res. Toxicol. 2013, 26, 1055−1063

units/mL penicillin G sodium; 10000 μg/mL streptomycin sulfate and 25 μg/mL amphotericin B in 0.85% saline (Gibco)]. The cells were incubated at 37 °C with 5% carbon dioxide, and logarithmically growing cells were used for all experiments.

MTT and TUNEL Assays. Cell viability was determined using the MTT assay. Cells were seeded at a density of 10^4 cells/100 μL of medium. HeLa and HepG2 cells were seeded into 96-microwell plates 12 h before being treated. The cells were treated with serial dilutions of the compounds in assay medium (DMEM), ranging from 4 to 0.004 μM. Cells treated with DMSO alone were used as controls. After incubation for 48 h, the supernatant was removed and 3-(4,5-dimethylthiazol-2-yl)-2,5-diphenyltetrazolium bromide (MTT) was added to each well at a final concentration of 2.5 mg/mL, followed by an additional incubation at 37 °C for 4 h. Subsequently, 100 μL of DMSO was added to each well, and after 20 min, the absorbance of each well was measured at 570 nm (Multiskan FC multiplate photometer, Thermo Scientific, Waltham, MA). The IC_{50} was calculated as the compound concentration required for the inhibition of 50% of the cell growth relative to the controls. Cisplatin and Taxol (Sigma, St. Louis, MO) were used as positive controls.

For the terminal deoxynucleotidyl transferase dUTP nick-end labeling (TUNEL) assay, HeLa cells were seeded onto the coverslips at a density of 10^5 cells/mL of medium. After being treated with citreamicin ε A (**1**) at 0.22 μM for 3, 6, and 9 h, the cells were washed with phosphate-buffered saline (PBS) three times and fixed with 4% paraformaldehyde (PFA) for 20 min at room temperature. After permeabilization in PBS containing 0.1% Triton X-100 and 0.1% sodium citrate, the fluorescein-based TUNEL assay (Roche Applied Science) was conducted according to the manufacturer's instructions. Briefly, HeLa cells were incubated in 50 μL of the TUNEL reaction mixtures containing label and enzyme solution for 60 min at 37 °C in the dark. After being washed twice with PBS, the cells were stained with Hoechst 33342 (Sigma) for 15 min. After the cells had been rinsed with PBS, the coverslips were mounted onto glass slides and the slides observed microscopically. The cells treated with DMSO alone were considered as negative controls.

Western Blot Analysis. HeLa cells at a density of 10^5 cells/mL of medium were treated with citreamicin ε A at a final concentration of 0.22 μM. The cells were collected at different time points (6, 9, 12, and 24 h) and lysed in lysis buffer [50 mM Tris-HCl (pH 7.8), 150 mM NaCl, 1% Triton X-100, and protease and phosphatase inhibitors]. Proteins (60 μg samples) were separated by 10% sodium dodecyl sulfate−polyacrylamide gel electrophoresis (SDS−PAGE) and transferred onto a Hybond ECL nitrocellulose membrane (Bio-Rad). After being blocked with 5% nonfat milk in Tris-buffered saline containing 0.1% Tween (TBST), the membranes were incubated with the primary antibodies overnight at 4 °C or for 2 h at room temperature. The membranes were washed with TBST three times at 15 min intervals and subsequently incubated with the horseradish peroxidase-conjugated secondary antibody at room temperature for 1 h. After incubation with the secondary antibody, the membranes were developed using Immobilon Western detection reagents (Millipore, Billerica, MA). The following primary antibodies were used in this study: anti-poly-ADP-ribose polymerase (PARP-1) (Santa Cruz), anti-caspase-3 (Santa Cruz), anti-Mcl-1 (Abcam), and anti-β-actin (Sigma-Aldrich).

Measurements of Intracellular Reactive Oxygen Species Levels. Intracellular ROS levels were determined using the molecular probe 2,7-dichlorofluorescein diacetate (DCFDA).[24] The nonpolar DCFDA probe crosses cell membranes and is hydrolyzed by intracellular esterases to its nonfluorescent form dichlorofluorescein (DCFH), which is subsequently oxidized to the highly fluorescent dichlorofluorescein (DCF) in the presence of ROS.[25] HeLa cells were seeded in black 96-well plates with clear bottoms at a density of 10^4 cells/100 μL of medium (Perkin-Elmer), rinsed twice with PBS, and incubated with DMEM containing 10 μM DCFDA (Fluka, Buche, Switzerland) at 37 °C for 30 min. After an additional rinse with PBS, the cells were incubated with fresh medium containing 0.43 μM citreamicin ε A and B or oxicitreamicin ε A and B in the presence or absence of 10 mM *N*-acetyl-L-cysteine (NAC) (Sigma-Aldrich). The fluorescence was measured immediately after addition of the compound using a multilabel counter (Victor V^2, Perkin-Elmer) at 37 °C with an excitation wavelength of 485 nm and an emission wavelength of 535 nm. The fluorescence values for each sample were recorded at 1 min intervals for the first 30 min and 1 h intervals for the subsequent 4 h.

Oxidation Reaction. The diastereomeric mixture (10 mg) was dissolved in THF (12 mL). Subsequently, 9.0 mg of silver oxide was added to this solution.[26] The mixture was stirred at room temperature for 48 h and filtered with filter paper. The filtrate was evaporated at a reduced pressure in a SpeedVac (Labconco Corp., Kansas City, MO), and the residue was dissolved in methanol for HPLC analysis (Figure S22 of the Supporting Information). The products of the reaction were subjected to semipreparative HPLC separation to purify oxicitreamicin ε A (**3**) (3.2 mg) and B (**4**) (2.9 mg).

RESULTS

^{1}H and ^{13}C NMR Signal Assignments. Citreamicin ε A (**1**) and B (**2**) were purified as optically active yellow powders. Analysis of the one-dimensional (1D) and 2D NMR spectra of citreamicin ε A (**1**) and B (**2**) confirmed the planar structures of these compounds, which were the same as the structure previously described for citreamicin ε. However, the stereochemical analysis of citreamicin ε remained ambiguous. A single crystal of citreamicin ε A (**1**) was obtained from a tetrahydrofuran (THF) solution and subjected to X-ray diffraction analysis. This is the first study to reveal the relative configurations of citreamicin ε, showing the same orientations of the methyl groups at positions C-3 and C-19 (Figure 2). The

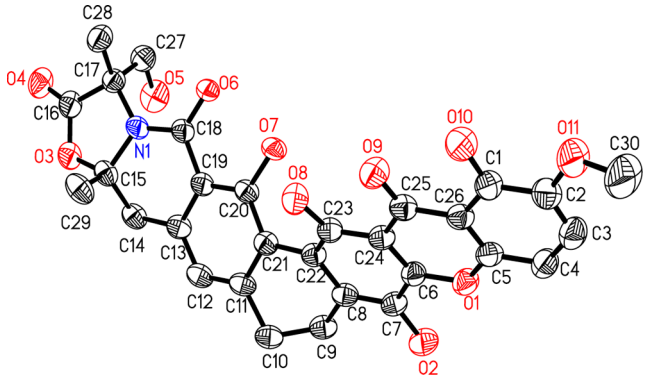

Figure 2. Oak Ridge Thermal Ellipsoid Plot (ORTEP) drawing of citreamicin ε A (**1**) obtained using X-ray diffraction.

relative configurations of citreamicin ε B (**2**) at positions C-3 and C-19 were determined using nuclear Overhauser effect spectroscopy (NOESY), conducted in acetone-d_6. The NOE correlation between H_3-21 (δ_H 1.68) and H-18 (δ_H 3.46) revealed the likelihood that these elements were located on the same side of the molecule, indicating that the methyl groups at positions C-3 and C-19 had an opposite orientation.

Cytotoxicity of Citreamicin ε A (1) and B (2) in HeLa and HepG2 Cells. The cytotoxic activity of citreamicin ε A (**1**) and B (**2**) against HeLa and HepG2 cells was evaluated *in vitro* using the MTT method. Both diastereomers displayed dose-dependent cytotoxic activity (Figure 3). Citreamicin ε A (**1**) and B (**2**) possessed IC_{50} values of 0.032 ± 0.0062 and 0.031 ± 0.0081 μM against HeLa cells and 0.079 ± 0.031 and 0.10 ± 0.0053 μM against HepG2 cells, respectively (Table 1), and this activity was approximately 100 times stronger than that demonstrated by the positive control Cisplatin.

dx.doi.org/10.1021/tx4000304 | *Chem. Res. Toxicol.* 2013, 26, 1055−1063

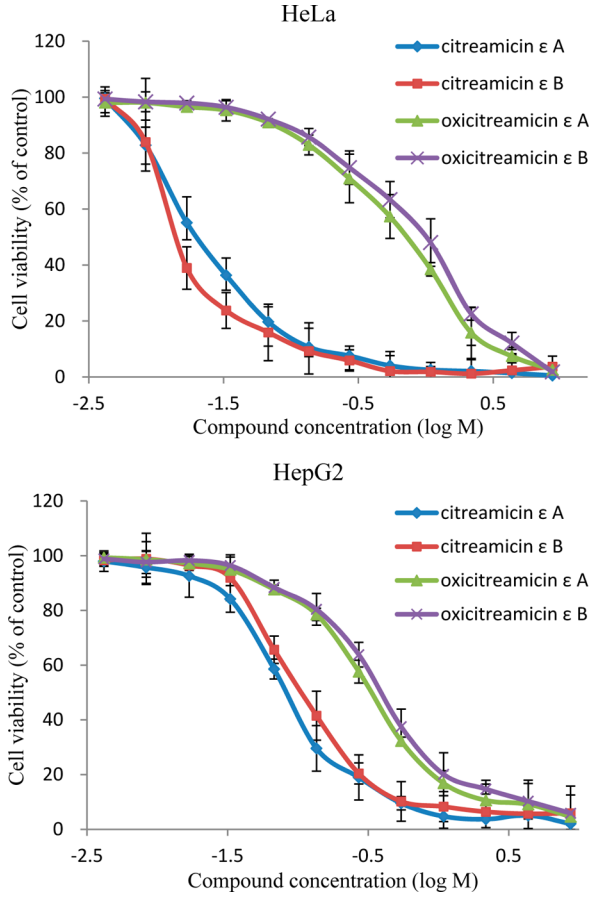

Figure 3. Citreamicin ε A (**1**) and B (**2**) and oxicitreamicin ε A (**3**) and B (**4**) had a dose-dependent effect on the viability of HeLa and HepG2 cells. HeLa and HepG2 cells were treated with different concentrations of these four compounds for 48 h, and cell viability was assessed using the MTT method. Data are presented as the mean ± SE of three independent experiments performed in triplicate.

Table 1. Cytotoxicity IC_{50} Values of Compounds 1−4 in Different Cell Lines

compound	HeLa (μM)	HepG2 (μM)
1	0.032 ± 0.0062	0.079 ± 0.031
2	0.031 ± 0.0081	0.10 ± 0.0053
3	0.56 ± 0.10	0.23 ± 0.031
4	0.76 ± 0.12	0.34 ± 0.071
Cisplatin[a]	9.1 ± 1.0	27 ± 1.7
Taxol[a]	0.00031 ± 0.00012	–[b]

[a]Positive control. [b]Did not test.

Citreamicin ε Induces HeLa Cell Apoptosis. To determine the potential cytotoxic mechanism of citreamicin ε in the HeLa cells, we used the TUNEL assay. This method specifically labels cleaved DNA in apoptotic cells with a green fluorescein-based nucleotide, whereas nonapoptotic cells with intact DNA remain unstained. The TUNEL assay has been used extensively to assess cell apoptosis.[27,28] Because there was no difference between these two diastereomers with respect to cytotoxic activity against HeLa cells, one of the diastereomers, citreamicin ε A (**1**), was selected to represent citreamicin ε. Hoechst 33342 was applied to detect all apoptotic or nonapoptotic cells. After a 3 h treatment with 0.22 μM citreamicin ε A (**1**), apoptosis was observed in approximately 4.29% of the cells. After a 6 h treatment, apoptosis was observed in approximately 11.2% of the cells, demonstrating a statistically significant, 2-fold greater increase in the level of apoptosis compared with that in the samples that were treated for 3 h. After treatment for 9 h, more than 70% of the cells were apoptotic, revealing 15- and 6-fold higher increases compared with those of the 3 and 6 h treatment samples, respectively. Apoptotic cells were scarce in the control samples (Figure 4). These data indicated that citreamicin ε A (**1**) induced apoptosis in HeLa cells in a time-dependent manner.

The Citreamicin ε-Induced Apoptosis of HeLa Cells Occurs through Activation of Cascade-3-Dependent Pathways. To further investigate whether the citreamicin ε A (**1**)-induced apoptosis of HeLa cells was mediated via the caspase-3 pathway, related proteins were evaluated by Western blot analysis. The results showed that the expression of inactivated caspase-3 (full-length) was downregulated in a time-dependent manner. After treatment with 0.22 μM citreamicin ε A (**1**) for 12 h, the level of caspase-3 expression was reduced to half of its original level, while the activated form of caspase-3 (cleaved) was upregulated after treatment for 9 h with citreamicin ε A (**1**), consistent with the change in full-length caspase-3. Activation of caspase-3 in cells treated with citreamicin ε A (**1**) was further confirmed using the substrate PARP (poly-ADP-ribose polymerase). The intact 116 kDa moiety of PARP-1 was degraded, and the cleaved fragment (89 kDa) was upregulated. After treatment for 24 h, almost half of the PARP-1 was cleaved, which was consistent with the expression of caspase-3, suggesting that the cell undergoes apoptosis through a caspase-3-dependent pathway. The expression level of Mcl-1 was downregulated almost 5-fold following treatment for 24 h compared with time zero, further confirming that citreamicin ε A induced apoptosis in HeLa cells (Figure 5).

Citreamicin ε A (1) Induced Intracellular ROS Generation. In this study, citreamicin ε was oxidized to oxicitreamicin ε in HeLa cells after 1 h (Figure S31 of the Supporting Information), suggesting that the para phenolic groups in citreamicin ε can be oxidized into quinone groups. Because this process often involves the generation of ROS,[29] we measured ROS levels in citreamicin ε A (**1**)-induced HeLa cells using the classic DCFDA method. When DCFDA was incubated with citreamicin ε A (**1**) at a concentration of 0.43 μM in the absence of HeLa cells, there was almost no ROS generation, suggesting that the compound itself does not affect ROS generation without cells (Figure S32 of the Supporting Information). However, in DCFDA-loaded cells, an increase in fluorescence was observed after treatment with citreamicin ε A (**1**) at a concentration of 0.43 μM. In as little as 30 min, citeamicin ε A (**1**) treatment induced a 40% increase in the level of ROS generation in HeLa cells. After 30 min, ROS levels reached saturation, and ROS production was inhibited by cotreatment of the cells with 10 mM NAC (Figure 6).

Oxidation of Citreamicin ε. To confirm whether ROS were involved in citreamicin ε-induced apoptosis, the oxidized products, oxicitreamicin ε A (**3**) and B (**4**), were obtained using a one-step reaction catalyzed by Ag_2O (Figure 7A).[26,30] The molecular formula of both oxidation products, compounds **3** and **4**, was determined to be $C_{30}H_{23}NO_{11}$ using the HRESIMS measurement (*m/z* 574.1345 $[M + H]^+$ for **3** and *m/z* 574.1324 $[M + H]^+$ for **4**). These molecular formulas differed from the molecular formula of compound **1** by <2 Da. The ^1H and ^{13}C NMR spectra of compounds **3** and **4** (Table S2 of the

dx.doi.org/10.1021/tx4000304 | Chem. Res. Toxicol. 2013, 26, 1055−1063

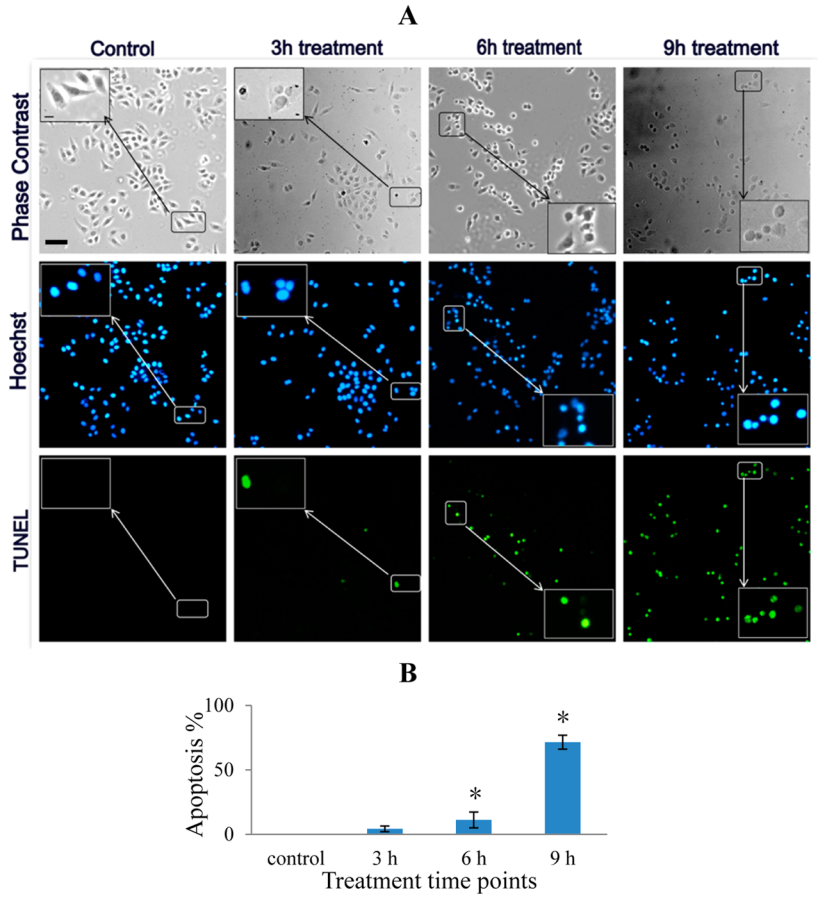

Figure 4. (A) Citreamicin ε A (**1**) induced HeLa cell apoptosis detected using a TUNEL assay. HeLa cells were treated for 3, 6, and 9 h with 0.22 μM citreamicin ε A (**1**). Scale bars are 50 μm; magnified scale bars are 10 μm. (B) Percentages of apoptotic cells calculated as the number of TUNEL-positive cells divided by the total number of cancer cells in each treatment. Values are presented as means ± SE of triplicate experiments. *$p < 0.05$.

Supporting Information) were similar to those recorded for compound **1**. Comparison of the ^{1}H and ^{13}C NMR spectra of compounds **1** and **3** revealed an absence of active hydrogen signals from the 7-OH and 14-OH groups and changes in the chemical shift at C-7 (δ_C 180.5) and C-14 (δ_C 178.5) in the 1D NMR spectra of compound **3**. These findings confirmed that in the planar structure of compound **3**, *p*-quinone groups replaced the phenolic groups present in citreamicin ε A (**1**). The ^{1}H and ^{13}C NMR spectra of compounds **3** and **4** were nearly identical. On the basis of these results, compounds **3** and **4** were considered diastereomers at the C-19 position, namely, oxicitreamicin ε A (**3**) and B (**4**), respectively.

Oxicitreamicin ε Induced a Decreased Level of Intracellular ROS Generation and Possessed Less Cytotoxic Activity Than Citreamicin ε. A 20% increase in the level of ROS generation was induced in HeLa cells using oxicitreamicin ε A (**3**), which contains a *p*-quinone group in ring C. This increase was 20% smaller than that observed in response to treatment with citreamicin ε A (**1**) (Figure 6). In the MTT assay, The IC_{50} values of oxicitreamicin ε A (**3**) and B (**4**) in HeLa cells were 0.56 ± 0.10 and 0.76 ± 0.12 μM, respectively (Table 1), demonstrating a cytotoxicity that was more than 15-fold weaker than that of citreamicin ε A (**1**) and B (**2**). Comparison of the cytotoxic activity of citreamicin ε and its oxidized products revealed an important role for free hydroxyl groups at C-7 and C-14 because the IC_{50} values of oxicitreamicin ε A (**3**) and B (**4**), which have *p*-quinone groups at C-7 and C-14 instead of phenolic groups, were remarkably larger than citreamicin ε A (**1**) and B (**2**).

DISCUSSION

Marine microorganisms, particularly culturable marine bacteria, constitute a vast resource for the identification of novel structures with various bioactivities. We have recently reported several new members of the citreamicin group produced by a Red Sea *Streptomyces* strain.[31] In addition, this bacterial species also produced an enormous amount of citreamicin ε, which has two chiral centers and thereby four stereoisomers. Different stereoisomers vary greatly in their ability to induce biological functions. For example, White et al. studied the effects of different stereoisomers of ketamine and showed that (*S*)-ketamine provided significantly better operating conditions with less spontaneous motor activity than (*R*)-ketamine.[32] We found that the portion of the structure containing the chiral centers might be crucial for cytotoxicity because citreaglycon A was approximately 1000-fold less active than citreamicin ε.[31] Thus, isolating the individual stereoisomers is important. In the study presented here, we isolated a pair of diastereomers and resolved their different configurations using crystallization and NMR spectral analysis. This is the first study to report the successful crystallization of the structure of citreamicins. Although the toxicity of the two diastereomers against HeLa and HepG2 cells was nearly equivalent, these compounds showed some degree of variance in Ptk2 cells. We are currently

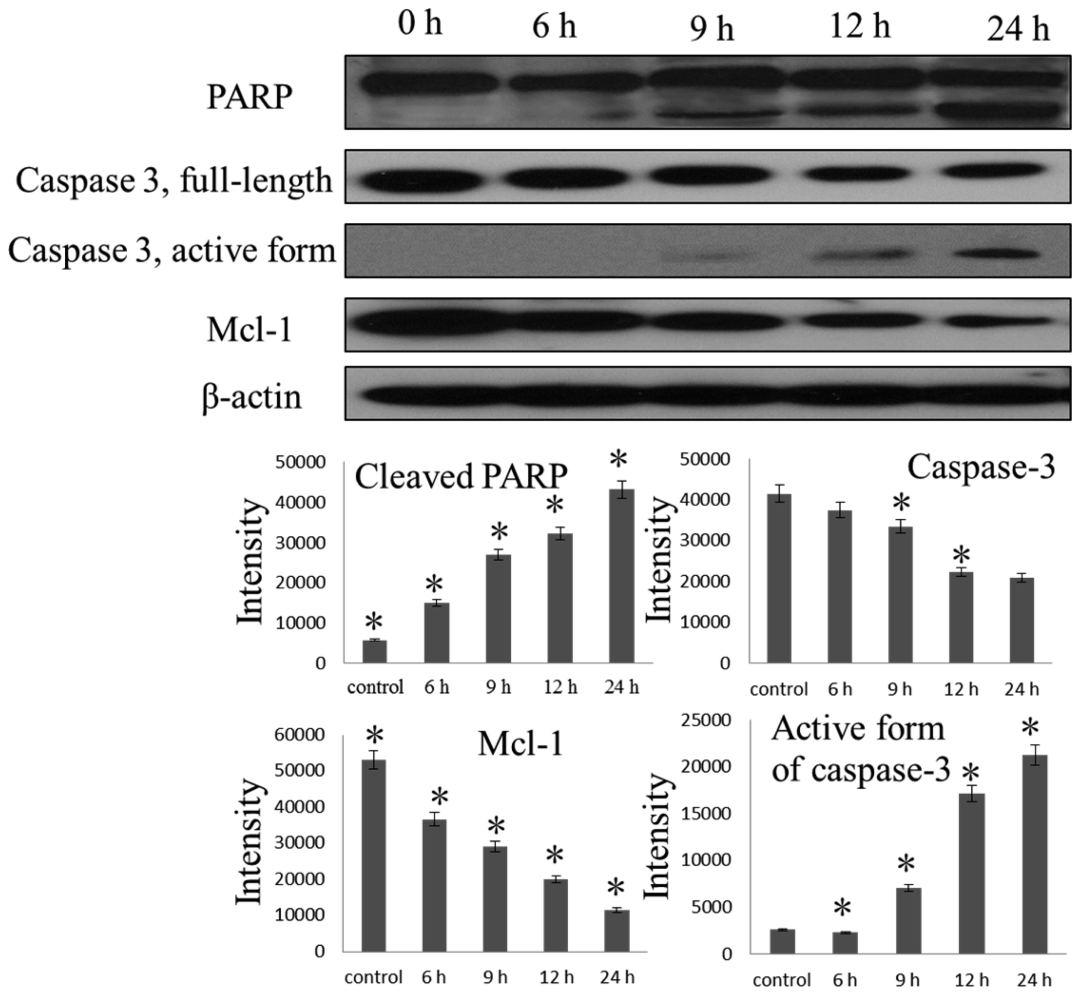

Figure 5. Caspase-3 activation in response to citreamicin ε A treatment of HeLa cells. Western blot analysis of PARP-1, caspase-3 (full-length and active forms), and Mcl-1 in HeLa cells treated with 0.22 μM citreamicin ε A (**1**) for 6, 9, 12, and 24 h. The intensity of each band was measured using ImageJ. Error bars represent the standard deviation of three separate experiments. *p < 0.05.

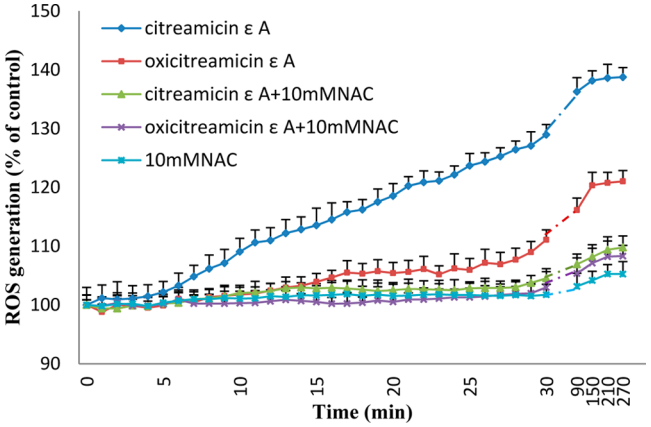

Figure 6. ROS production after treatment with citreamicin ε A (**1**) and oxicitreamicin ε A (**3**) at 0.43 μM for 270 min in the presence and absence of NAC, as monitored using DCF fluorescence. NAC alone served as a control. Each symbol represents the mean ± SE value of 34 observations.

using proteomics methods to investigate the mechanism underlying these observations.

Citreamicin was recently patented as an antitumor drug lead because of its outstanding cytotoxic activity,[20] yet the mode of action of this compound remains unclear. Using a TUNEL assay, we observed that citreamicin ε induced DNA damage in HeLa cells. In most cases, DNA is the main target of cytotoxic anticancer drugs, which directly or indirectly bind to DNA or block its metabolic functions, such as the activity of DNA polymerases and/or topoisomerases.[33] Following DNA damage, apoptosis occurs. Apical caspase activation or putative cytosolic substrate cleavage has been recognized as solid evidence of apoptosis. In this study, downregulation of full-length caspase-3 and upregulation of its cleaved form together with cleaved PARP-1 in HeLa cells treated with citreamicin ε A (**1**) revealed citreamicin ε-induced apoptosis occurred through the caspase-3-dependent pathway. Furthermore, Mcl-1, which belongs to the Bcl-2 family, is an essential survival protein that is classified as an anti-apoptotic protein. Cells display the most dramatic induction of apoptosis when there is a reduced level of Mcl-1 protein.[34] Thus, the observed downregulation of the Mcl-1 protein further confirmed that HeLa cell apoptosis was induced by citreamicin ε A (**1**).

The cytotoxic activity of citreamicin ε may be due to caspase-3-dependent apoptosis. Many factors can trigger cell apoptosis, such as ROS production. Excessive ROS can cause oxidative damage to proteins, lipids, and respiratory chain proteins, and ROS can activate caspases and other apoptotic factors.[35,36] ROS are also considered as stimuli for both intrinsic and extrinsic

dx.doi.org/10.1021/tx4000304 | Chem. Res. Toxicol. 2013, 26, 1055−1063

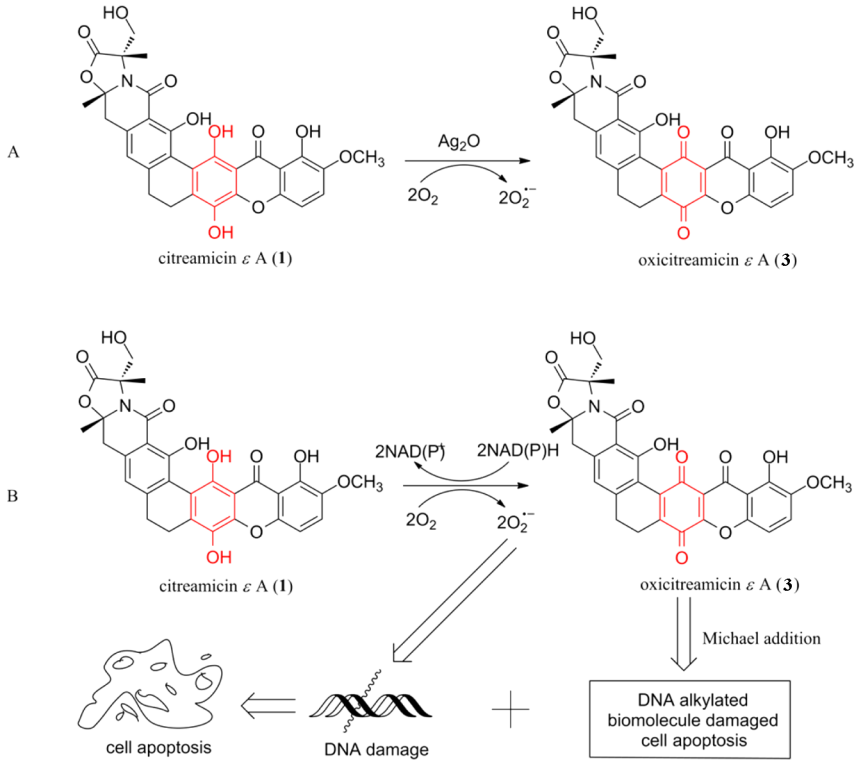

Figure 7. (A) Oxidative reaction of citreamicin ε catalyzed by Ag_2O. (B) Predicted ROS generation mediated by citreamicin ε treatment *in vitro*, leading to DNA damage and apoptosis.

apoptosis pathways. Stimulation of the intrinsic mitochondrial apoptotic pathway through ROS triggers caspase-dependent or caspase-independent cytosolic signaling events.[37] Recent evidence suggests a possible direct role for ROS in mediating death receptor activation and apoptotic induction in the extrinsic apoptotic pathway.[38,39] Under oxidative stress, tumor cells might have a limited capacity to adapt to some environmental changes; therefore, antitumor agents that induce the generation of ROS have potential therapeutic benefits.[40]

In this study, we observed that citreamicin ε increased the level of intracellular ROS by 40% compared with the normal level in HeLa cells, which is a significant increase in the level of ROS production. To determine whether ROS was indeed involved in the cytotoxicity of citreamicin ε, we oxidized citreamicin ε into oxicitreamicin ε and observed a 20% increase in the level of intracellular ROS, which was 20% lower than that observed with citreamicin ε. The cytotoxicity of oxicitreamicin ε was also substantially reduced. The difference in ROS generation between these two compounds reflected differences in cytotoxicity. Moreover, oxicitreamicin ε was detected in HeLa cells after they had been treated with citreamicin ε for 1 h. On the basis of a comparative analysis of the chemical structures of citreamicin ε and oxicitreamicin ε, we proposed two hypotheses. (1) The *p*-hydroxyl groups on ring C in citreamicin ε A (**1**) are converted into *p*-quinone groups *in vivo*, leading to the formation of ROS (Figure 7B).[28] (2) Both citreamicin ε and oxicitreamicin ε may bind to the key enzyme via hydrogen bonding. With regard to the first hypothesis, it has been shown that excess intracellular ROS is associated with DNA damage and cell apoptosis and that it might contribute partially to the cytotoxic activity of citreamicin ε A (**1**). Conjugation of the ligand to the protein may trigger the apoptosis pathway as well as the ROS production pathway in the cell, whereas the different toxicities of citreamicin ε and oxicitreamicin ε may due to differences in binding affinity. To investigate which hypothesis is more convincing, we conducted rescue experiments. ROS generation was significantly inhibited by NAC; however, there were no differences in cell viability in response to citreamicin ε treatment in the presence and absence of NAC.

The *p*-quinone groups in oxicitreamicin ε might play an important role in the cytotoxicity of this compound. Quinones are cytotoxic because of their ability to damage biomolecules through alkylation via a Michael addition.[41] This process activates or inhibits protein responses, which has a prominent impact on apoptosis. Quinones, as Michael acceptors, sometimes induce cell damage through covalent binding with cellular nucleophiles such as the nucleophilic amino groups that are present on proteins or DNA.[42] For example, *p*-benzoquinone forms a DNA adduct that induces cell apoptosis.[43] Oxicitreamicin ε, with a *p*-quinone in ring C, might have a cytotoxic mechanism similar to that of quinones.

The five-member heterocyclic ring might also contribute to the cytotoxic activity of citreamicins, as this molecule is similar to oxazolines, a class of antibiotics that function as protein synthesis inhibitors.[44] Nitrogen- and oxygen-containing heterocycles, such as oxazolines, are important for biologically active compounds. In a previous study, we observed that compounds without this five-member heterocyclic ring display much lower cytotoxic activity than citreamicin, consistent with our hypothesis.

■ CONCLUSION

We found that when strain *S. caelestis* was grown in a flask containing glass beads, it yielded a large amount of citreamicin ε. We isolated and determined the relative configuration of a

dx.doi.org/10.1021/tx4000304 | *Chem. Res. Toxicol.* 2013, 26, 1055−1063

pair of diastereomers, citreamicin ε A (**1**) and B (**2**). Both diastereomers possessed strong cytotoxic activities against HeLa and HepG2 cells. HeLa cells treated with citreamicin ε A (**1**) displayed DNA fragmentation and caspase-3-dependent cell apoptosis. Citreamicin ε A (**1**) greatly increased the intracellular ROS concentration in HeLa cells, suggesting the possible involvement of ROS in cell apoptosis. Oxicitreamicin ε, the oxidized product of citreamicin ε with a weakened ability to promote ROS generation, was also less cytotoxic than citreamicin ε. The ROS scavenger NAC could reduce the level of ROS generation in cotreatment assays with citreamicin ε, but it could not protect HeLa cells against the cytotoxicity of citreamicin ε.

■ ASSOCIATED CONTENT

Ⓢ Supporting Information

1D and 2D NMR, IR, and HRESIMS spectra for compounds **1**−**4** and the parallel experimental results for the two diastereomers. This material is available free of charge via the Internet at http://pubs.acs.org.

■ AUTHOR INFORMATION

Corresponding Author

*E-mail: boqianpy@ust.hk.

Author Contributions

L.-L.L. and L.-S.H. contributed equally to this work.

Funding

This work was supported by a research grant (DY125-15-T-02) from the China Ocean Mineral Resources Research and Development Association and by Grant SA-C0040/UK-C001 from King Abdullah University of Science and Technology (KAUST) to P.-Y.Q.

Notes

The authors declare no competing financial interest.

■ ACKNOWLEDGMENTS

We are grateful to Rui Feng (Division of Life Sciences, Hong Kong University of Science and Technology) for the NMR spectra. We also thank Ms. Soumaya Belkharchouche for proofreading the manuscript and Dr. Chen Na for the ROS measurements.

■ ABBREVIATIONS

ROS, reactive oxygen species; H_2O_2, hydrogen peroxide; EA, ethyl acetate; DMSO, dimethyl sulfoxide; DMEM, Dulbecco's modified Eagle's medium; FBS, fetal bovine serum; MTT, 3-(4,5-dimethylthiazol-2-yl)-2,5-diphenyltetrazolium bromide; TUNEL, terminal deoxynucleotidyl transferase dUTP nick-end labeling; PFA, paraformaldehyde; TBST, Tris-buffered saline with 0.1% Tween; PARP-1, poly-ADP-ribose polymerase; NOESY, nuclear Overhauser effect spectroscopy; DCFDA, 2,7-dichlorofluorescein diacetate; DCFH, dichlorofluorescein; DCF, dichlorofluorescein; NAC, *N*-acetyl-L-cysteine

■ REFERENCES

(1) Carter, G. T., Nietsche, J. A., Williams, D. R., and Borders, D. B. (1990) Citreamicins, novel antibiotics from *Micromonospora citrea*: Isolation, characterization, and structure determination. *J. Antibiot. 43*, 504−512.

(2) Carter, G. T., Borders, D. B., Goodman, J. J., Ashcroft, J., Greenstein, M., Maiese, W. M., and Pearce, C. J. (1991) Biosynthetic origins of the polycyclic xanthone antibiotic, citreamicin. *J. Chem. Soc., Perkin Trans. 1 9*, 2215−2219.

(3) Reich, M. F., Lee, V. J., Ashcroft, J., and Morton, G. O. (1993) An unusual cyclization product from the reaction of citreamicin η with sulfene. *J. Org. Chem. 58*, 5288−5290.

(4) Peoples, A. J., Zhang, Q., Millett, W. P., Rothfeder, M. T., Pescatore, B. C., Madden, A. A., Ling, L. L., and Moore, C. M. (2009) Neocitreamicins I and II, Novel Antibiotics with Activity against Methicillin-Resistant *Staphylococcus aureus* and Vancomycin-Resistant *Enterococci*. *J. Antibiot. 61*, 457−463.

(5) Hopp, D. C., Milanowski, D. J., Rhea, J., Jacobsen, D., Rabenstein, J., Smith, C., Romari, K., Clarke, M., Francis, L., Irigoyen, M., Luche, M., Carr, G. J., and Mocek, U. (2008) Citreamicins with Potent Gram-Positive Activity. *J Nat. Prod. 71*, 2032−2035.

(6) Vaux, D. L., and Korsmeyer, S. J. (1999) Cell death in development. *Cell 96*, 245−254.

(7) Sun, X. M., MacFarlane, M., Zhuang, J., Wolf, B. B., Green, D. R., and Cohen, G. M. (1999) Distinct caspase cascades are initiated in receptor-mediated and chemical-induced apoptosis. *J. Biol. Chem. 274*, 5053−5060.

(8) Desagher, S., and Martinou, J. C. (2000) Mitochondria as the central control point of apoptosis. *Trends Cell Biol. 10*, 369−377.

(9) McConkey, D. J. (1998) Biochemical determinants of apoptosis and necrosis. *Toxicol. Lett. 99*, 157−168.

(10) Elmore, S. (2007) Apoptosis: A Review of Programmed Cell Death. *Toxicol. Pathol. 35*, 495−516.

(11) Kamradt, M. C., Chen, F., and Cryns, V. L. (2001) The Small Heat Shock Protein αB-Crystallin Negatively Regulates Cytochrome c and Caspase-8-dependent Activation of Caspase-3 by Inhibiting Its Autoproteolytic Maturation. *J. Biol. Chem. 276*, 16059−16063.

(12) Circu, M. L., and Aw, T. Y. (2010) Reactive oxygen species, cellular redox systems, and apoptosis. *Free Radical Biol. Med. 48*, 749−762.

(13) Jones, D. C., Gunasekar, P. G., Borowitz, J. L., and Isom, G. E. (2000) Dopamine-Induced Apoptosis Is Mediated by Oxidative Stress and Is Enhanced by Cyanide in Differentiated PC12 Cells. *J. Neurochem. 74*, 2296−2304.

(14) Circu, M. L., Moyer, M. P., Harrison, L., and Aw, T. Y. (2009) Contribution of glutathione status to oxidant-induced mitochondrial DNA damage in colonic epithelial cells. *Free Radical Biol. Med. 47*, 1190−1198.

(15) Rachek, L. I., Yuzefovych, L. V., Ledoux, S. P., Julie, N. L., and Wilson, G. L. (2009) Troglitazone, but not rosiglitazone, damages mitochondrial DNA and induces mitochondrial dysfunction and cell death in human hepatocytes. *Toxicol. Appl. Pharmacol. 240*, 348−354.

(16) Li, P. F., Dietz, R., and Vonharsdorf, R. (1997) Differential effect of hydrogen peroxide and superoxide anion on apoptosis and proliferation of vascular smooth muscle cells. *Circulation 96*, 3602−3609.

(17) Rauen, U., and Degroot, H. (1998) Cold-induced release of reactive oxygen species as a decisive mediator of hypothermia injury to cultured liver cells. *Free Radical Biol. Med. 24*, 1316−1323.

(18) Inayat-Hussain, S. H., and Ross, D. (2005) Intrinsic Pathway of Hydroquinone Induced Apoptosis Occurs via Both Caspase-Dependent and Caspase-Independent Mechanisms. *Chem. Res. Toxicol. 18*, 420−427.

(19) Marshall, K. M., and Barrows, L. R. (2004) Biological activities of pyridoacridines. *Nat. Prod. Rep. 21*, 731−751.

(20) Puentes, F., Fernandez, C., Gravalos, G., Baz, P., Millan, R., and Vazquez, E. (2003) New use of citreamicins. EP1292299.

(21) Sambrook, J., Fritsch, E. F., and Maniatis, T. (1989) *Molecular Cloning. A Laboratory Manual*, 2nd ed., pp 914−923, Cold Spring Harbor Laboratory Press, Plainview, NY.

(22) Altschul, S. F., Madden, T. L., Schäffer, A. A., Zhang, J., Zhang, Z., Miller, W., and Lipman, D. J. (1997) Gapped BLAST and PSI-BLAST: A new generation of protein database search programs. *Nucleic Acids Res. 25*, 3389−3402.

(23) Crystallographic data for citreamicin ε A (**1**) reported in this paper have been deposited with the Cambridge Crystallographic Data

Centre with deposition number 890247. Copies of the data can be obtained free of charge on application to the Director CCDC, 12 Union Road, Cambridge CB2 IEZ, U.K. [fax, +44-(0) 1223−336033; or e-mail, deposit@ccdc.cam.ac.uk].
(24) Wang, H., and Joseph, J. A. (1999) Quantifying cellular oxidative stress by dichlorofluorescein assay using microplate reader. *Free Radical Biol. Med. 27*, 612−616.
(25) Lebel, C. P., Ischiropoulos, H., and Bondy, S. C. (1992) Evaluation of the probe 2′,7′-dichlorofluorescein as an indicator of reactive oxygen species formation and oxidative stress. *Chem. Res. Toxicol. 5*, 227−231.
(26) Angle, S. R., Rainier, J. D., and Woytowicz, C. (1997) Synthesis and Chemistry of Quinone Methide Models for the Anthracycline Antitumor Antibiotics. *J. Org. Chem. 62*, 5884−5892.
(27) Darzynkiewicz, Z., Galkowski, D., and Zhao, H. (2008) Analysis of apoptosis by cytometry using TUNEL assay. *Methods 44*, 250−254.
(28) Rohwer, F., and Azam, F. (2000) Detection of DNA damage in prokaryotes by terminal deoxyribonucleotide transferase-mediated dUTP nick end labeling. *Appl. Environ. Microbiol. 66*, 1001−1006.
(29) Bolton, J. L., Trush, M. A., Penning, T. M., Dryhurst, G., and Monks, T. J. (2000) Role of quinones in toxicology. *Chem. Res. Toxicol. 13*, 135−160.
(30) Valderrama, J. A., Colonelli, P., Vasquez, D., Gonzalez, M. F., Rodriguez, J. A., and Theoduloz, C. (2008) Studies on quinones. Part 44: Novel angucyclinone N-heterocyclic analogues endowed with antitumoral activity. *Bioorg. Med. Chem. 16*, 10172−10181.
(31) Liu, L.-L., Xu, Y., Han, Z., Li, Y.-X., Lu, L., Lai, P.-Y., Zhong, J.-L., Guo, X.-R., Zhang, X.-X., and Qian, P.-Y. (2012) Four New Antibacterial Xanthones from the Marine-Derived Actinomycetes *Streptomyces caelestis*. *Mar. Drugs 10*, 2571−2583.
(32) White, P. F., Ham, J., Way, W. L., and Trevor, A. (1980) Pharmacology of ketamine isomers in surgical patients. *Anesthesiology 52*, 231−239.
(33) Roos, W. P., and Kaina, B. (2006) DNA damage-induced cell death by apoptosis. *Trends Mol. Med. 12*, 440−450.
(34) Han, J., Goldstein, L. A., Gastman, B. R., Rabinovitz, A., and Rabinowich, H. (2005) Disruption of Mcl-1 Bim Complex in Granzyme B-mediated Mitochondrial Apoptosis. *J. Biol. Chem. 280*, 16383−16392.
(35) Monks, T. J., Hanzlik, R. P., Cohen, G. M., Ross, D., and Graham, D. G. (1992) Quinone chemistry and toxicity. *Toxicol. Appl. Pharmacol. 112*, 2−16.
(36) O'Brien, P. J. (1991) Molecular mechanisms of quinone cytotoxicity. *Chem.-Biol. Interact. 80*, 1−41.
(37) Ryter, S. W., Kim, H. P., Hoetzel, A., Park, J. W., Nakahira, K., Wang, X., and Choi, A. M. (2007) Mechanisms of cell death in oxidative stress. *Antioxid. Redox Signaling 9*, 49−89.
(38) Zhang, A. Y., Yi, F., Zhang, G., Gulbins, E., and Li, P.-L. (2006) Lipid Raft Clustering and Redox Signaling Platform Formation in Coronary Arterial Endothelial Cells. *Hypertension 47*, 74−80.
(39) Zhang, A. Y., Yi, F., Jin, S., Xia, M., Chen, Q. Z., Gulbins, E., and Li, P. L. (2007) Acid sphingomyelinase and its redox amplification in formation of lipid raft redox signaling platforms in endothelial cells. *Antioxid. Redox Signaling 9*, 817−828.
(40) Schafer, F. Q., and Buettner, G. R. (2001) Redox environment of the cell as viewed through the redox state of the glutathione disulfide/glutathione couple. *Free Radical Biol. Med. 30*, 1191−1212.
(41) Hirakawa, K., Oikawa, S., Hiraku, Y., Hirosawa, I., and Kawanishi, S. (2002) Catechol and Hydroquinone Have Different Redox Properties Responsible for Their Differential DNA-damaging Ability. *Chem. Res. Toxicol. 15*, 76−82.
(42) Nutter, L. M., Wu, Y. Y., Ngo, E. O., Sierra, E. E., Gutierrez, P. L., and Abul-Hajj, Y. J. (1994) An o-quinone form of estrogen produces free radicals in human breast cancer cells: Correlation with DNA damage. *Chem. Res. Toxicol. 7*, 23−28.
(43) Levay, G., Pongracz, K., and Bodell, W. J. (1991) Detection of DNA adducts in HL-60 cells treated with hydroquinone and p-benzoquinone by ^{32}P-postlabeling. *Carcinogenesis 12*, 1181−1186.
(44) Shinabarger, D. (1999) Mechanism of action of the oxazolidinone antibacterial agents. *Expert Opin. Invest. Drugs 8*, 1195−1202.